Detection of Tl(I) Transport through a Gramicidin−Dioleoylphosphatidylcholine Monolayer Using the Substrate Generation−Tip Collection Mode of Scanning Electrochemical Microscopy

J. Mauzeroll, M. Buda, and A. J. Bard*

Department of Chemistry & Biochemistry, The University of Texas at Austin, Austin, Texas 78722

F. Prieto and M. Rueda

Department of Physical Chemistry, University of Sevilla, Sevilla 41012, Spain

Received July 19, 2002. In Final Form: September 20, 2002

We report the use of scanning electrochemical microscopy (SECM) to control the generation of Tl(I) at a mercury substrate and detect this species at a mercury-coated tip to study the transport of these ions through ion channels. The transport of Tl(I) across gramicidin D half-channels imbedded in a dioleoylphosphatidylcholine (DOPC) monolayer supported on a Tl amalgam hanging mercury drop electrode (HMDE) was studied using the substrate generation−tip collection mode of SECM. A Hg/Pt "submarine" electrode, used as the SECM tip, was made through simple contact of the Pt ultramicroelectrode with the HMDE. The tip transient response for the collection of generated Tl(I) at the amalgam HMDE was recorded for several tip to substrate distances. This collection−generation experiment was repeated with a DOPC-modified Tl/HMDE and a gramicidin−DOPC-modified Tl/HMDE. An apparent heterogeneous rate constant (k_{het} = 2.8 (±0.1) × 10^{-4} cm/s) for the transport of Tl(I) through the gramicidin to the tip was extracted.

1. Introduction

The theory[1−3] and applications of scanning electrochemical microscopy (SECM) have been discussed elsewhere.[4] Most SECM measurements involve steady-state current measurements. However, transient current measurements have also been performed and provide information about the kinetics of homogeneous reactions and time-dependent systems. SECM transient response has previously been simulated and experimentally observed for planar electrodes, microdisks, and thin-layer cells over a wide time range.[5] When the tip radius is known, transient current measurements allow for the determination of diffusion coefficients without knowledge of solution concentration and the number of electrons transferred. This concept was also corroborated by later work.[6] In the substrate generation−tip collection (SG−TC) SECM mode, the substrate generates an electroactive species that diffuses into the bulk. An ultramicroelectrode (UME) positioned close to the substrate collects the generated species. The tip is at least an order of magnitude smaller than the substrate and has a thinner diffusion layer than the substrate. The tip reaction therefore does not significantly affect the substrate current.

Generation−collection experiments with an amperometric tip were pioneered by Engstrom et al.,[7−9] where a small carbon UME was employed to collect and study species generated at a nearby macroscopic electrode. They addressed the theoretical behavior of the tip transient response using potential step functions and impulse response functions and showed how this collection mode could be used for the collection of short-lived species, such as nicotinamide adenine dinucleotide (NAD) and epinephrine. They also studied the response time of a Nafion-coated UME in generation−collection experiments. The imaging capabilities of SECM in a SG−TC mode have also been used to monitor the activity of enzyme-modified microstructures.[10,11]

The diversity of membrane structures and transport mechanisms studied by SECM demonstrates the utility of this technique for studies of membrane transport. Diffusion across porous mica[12] or dentine[13]and iontophoresis across skin[14] are all examples of SECM studies of molecular transport across membranes. Previous work by our group used ion-selective micropipet electrodes in the SECM feedback and SG−TC modes to study K(I) transport through gramicidin D channels in a horizontal bilayer lipid membrane.[15,16]As we describe here, Tl(I) can

* To whom correspondence should be addressed.

(1) Kwak, J.; Bard, A. J. *Anal. Chem.* **1989**, *61*, 1221.
(2) Bard, A. J.; Fan, F.-R. R.; Kwak, J.; Lev, O. *Anal. Chem.* **1989**, *61*, 132.
(3) Davis, J. M.; Fan, F.-R. R.; Bard, A. J. *J. Electroanal. Chem. Interfacial Electrochem.* **1987**, *238*, 9.
(4) Bard, A. J.; Mirkin, M. V. In *Scanning Electrochemical Microscopy*; Marcel Dekker: New York, 2001.
(5) Bard, A. J.; Denuault, G.; Friesner, R. A.; Dornblaser, B. C.; Tuckerman, L. S.; *Anal. Chem.* **1991**, *63*, 1282.
(6) Martin, R. D.; Unwin, P. R. *Anal. Chem.* **1998**, *70*, 276.
(7) Engstrom, R. C.; Weber, M.; Wunder, D. J.; Burgess, R.; Winquist, S. *Anal. Chem.* **1986**, *58*, 844.
(8) Engstrom, R. C.; Meaney, T.; Tople, R.; Wightman, R. M. *Anal. Chem.* **1987**, *59*, 2005.
(9) Engstrom, R. C.; Wightman, R. M.; Kristensen, E. W. *Anal. Chem.* **1988**, *60*, 652.
(10) Kranz, C.; Wittstock, G.; Wohlschläger, H.; Schuhmann, W. *Electrochem. Acta* **1997**, *42*, 3105.
(11) Wittstock, G.; Schuhmann, W. *Anal. Chem.* **1997**, *69*, 5059.
(12) Scott, E. R.; White, H. S.; Phipps, J. B. *J. Membr. Sci.* **1991**, *58*, 71.
(13) Macpherson, J. V.; Beeston, M. A.; Unwin, P. R.; Hughes, N. P.; Littlewood, D. *J. Chem. Soc., Faraday Trans.* **1995**, *91*, 1407.
(14) Scott, E. R.; Phipps, J. B.; White, H. S. *J. Invest. Dermatol.* **1995**, *104*, 142.
(15) Amemiya, S.; Bard, A. J. *Anal. Chem.* **2000**, *72*, 4940.
(16) Amemiya, S.; Ding, Z.; Zhou, J.; Bard, A. J. *Electro. Chem.* **2000**, *483*, 7.

10.1021/la0262710 CCC: $22.00
Published on Web 11/02/2002

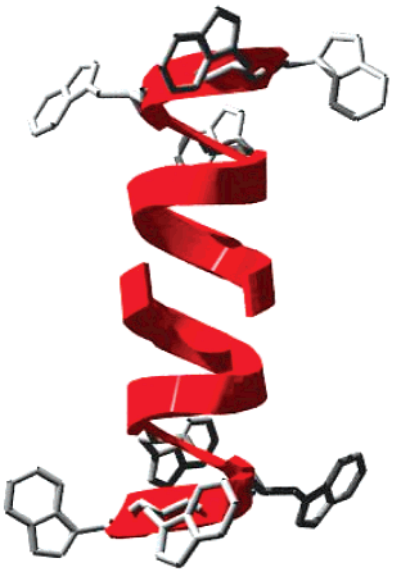

Figure 1. Full-channel image of gramicidin A outlining the position of the four tryptophan groups at each extremity of the dimer. The reported structure was reproduced based on solid NMR studies (refs 43 and 44).

be used as a surrogate for K(I), so that ion transport across gramicidin channels can be monitored using an amperometric UME rather than an ion-selective probe. It also allows one to control the release of the Tl(I) into the gramicidin channels by preconcentration of the Tl as an amalgam on a hanging mercury drop electrode (HMDE) with controlled oxidation of the amalgam using a potential step. A Hg/Pt submarine UME positioned close to the HMDE collects the generated Tl(I) following its diffusion from the substrate to tip. The tip collection response for different tip to substrate separations was evaluated. The response for the bare HMDE at a known tip to substrate distance was then compared to that of a dioleoylphosphatidylcholine (DOPC) and gramicidin−DOPC amalgamated HMDE.

Phospholipid-coated mercury electrodes with incorporated gramicidin have previously been used as membrane models.[17] The phospholipids form an organized monolayer at the Hg surface, where the tail of the lipid faces the mercury and the polar headgroups face the electrolyte solution.[18−20] When gramicidin channels are inserted into the DOPC monolayer, the conduction of Tl(I) ions is found over a potential region where the layer is usually ion impermeable.[21] Gramicidin is a linear 15 amino acid peptide synthesized by *Bacillus brevis* that is often used as a model ion channel for monovalent cations (Figure 1). It is composed of alternating D and L amino acids. The primary sequence of gramicidin A starting from the N terminal is HCO-val-gly-L-ala-D-leu-L-ala-D-val-L-val-D-val-L-trp-D-leu-L-*trp*-D-leu-L-trp-D-leu-L-trp-$NHCH_2CH_2$-OH. The italicized amino acid accounts for the natural variants of gramicidin (gram A (trp), gram B (phe), gram C (tyr)[22]) that make up gramicidin D in a 80:15:5 ratio, respectively. A full gramicidin channel (2.6−3 nm diameter) is formed from a dimer composed of two $\beta^{6.3}$ helices. A full channel is probably not present in a DOPC monolayer, since the thickness of the layer is only half that of a full channel. The Tl(I) conduction observed in the studied system is thus provided by a half-channel whose length is similar to that of the monolayer.[19,23] The effects of gramicidin concentration and choice of supporting electrolyte on the conduction of these half-channels have also been reported for this system.[24]

2. Experimental Section

2.1. Solution Preparation. All solutions and liquids were kept in glass containers previously washed overnight in saturated NaOH in EtOH and rinsed in water. The supporting electrolytes used were 0.1 M KCl solutions buffered with a 1:1 molar ratio of NaH_2PO_4/Na_2HPO_4 of total concentration 0.01 M at pH 7 (Mallinckrodt AR, Paris, KY). The redox couples employed were 2 mM hexaminеruthenium(III) chloride (Strem Chem., Newburyport, MA) and Tl(I) nitrate (Aldrich). The stock solution was 0.1 M Tl(I) nitrate with a Tl(I) concentration in the reaction cell of 0.1 mM. All solutions were prepared with Milli-Q (Millipore Corp.) reagent water and degassed with Ar for 30 min prior to all experiments.

A 0.1% stock solution of DOPC (Lipid Products, Nutfield, U.K.) in pentane (EM Sciences, Gibbstown, NJ) was stored at temperatures below −20 °C. A stock solution of 2.2 mM gramicidin D (Sigma) was prepared in methanol (EM Sciences) and stored in the refrigerator. Both solutions were stored in brown glass bottles with a Teflon cap (VWR Sci. Prod., Siwanee, GA).

2.2. SECM Apparatus. A CHI model 900 scanning electrochemical microscope (CH Instruments, Austin, TX) was used to control the tip potentials, obtain the approach curves, and monitor the tip to substrate distance. A battery-operated, home-built, floating potentiostat was used for potential control of the HMDE to prevent electrical coupling with the SECM in generation−collection experiments. The commercial SECM experienced electrical coupling during SG−TC transient experiments at short tip to substrate distances. This led to the superimposition of long current transients onto the tip collection response. In addition, the cell stage was modified to accommodate a chamber designed to allow measurements under oxygen-free conditions.

2.3. Electrodes. A 25 μm diameter Pt wire (Goodfellow, Cambridge, U.K.) was sealed into a 5 cm Pyrex glass capillary under a vacuum as described previously.[2] The electrode was polished and shaped into a UME on a polishing wheel (Buehler, Lake Bluff, IL) with 180 grid Carbimet paper disks (Buehler) and micropolishing cloth with 1.0, 0.3, and 0.05 μm alumina (Buehler). The tip was sharpened to an RG of 3, where RG is the ratio of the diameter of the UME that includes the glass sheet and the diameter of the Pt wire. The UME was then sealed into a J glass tube using Teflon tape to form the submarine electrode shown in Figure 2. The Hg/Pt UME was formed by applying −1.1 V to the Pt UME and making contact with the mercury (Bethlehem Instr., Hellertown, PA) of the hanging mercury drop electrode (Metrohm Instr., Herisau, Switzerland) in phosphate buffer.[25]

A 0.5 mm Pt wire (Goodfellow) and Hg/Hg_2SO_4 (Radiometer, Copenhagen, Denmark) electrode were used as counter and reference electrodes, respectively. All potentials are reported versus Hg/Hg_2SO_4.

2.4. Procedure. All experiments are performed sequentially in the same reaction vessel, a 750 mL cut beaker with a machined Teflon cap with an O-ring (Figure 2). The cap accommodated the HMDE, the submarine electrode, the reference and auxiliary electrodes, a gas inlet, and a microsyringe. An argon blanket was maintained over the solution at all times. The reaction vessel was filled with 250 mL of phosphate buffer and closed with all electrodes in place. The solution was purged with argon for 30 min. The tip and HMDE were aligned for the formation of the Hg/Pt UME. The tip was then retracted from the HMDE to a

(17) Nelson, A. *Biophys. J.* **2001**, *80*, 2694.
(18) Miller, I. R.; Rishpon, J.; Tenenbaum, A. *Bioelectrochem. Bioenerg.* **1976**, *3*, 528.
(19) Nelson, A.; Auffret, N. *J. Electroanal. Chem.* **1988**, *244*, 99.
(20) Nelson, A.; Leermarkers, F. A. M. *J. Electroanal. Chem.* **1990**, *278*, 73.
(21) Nelson, A.; Bizzotto, D. *Langmuir* **1999**, *15*, 7031.
(22) Woolley, G. A.; Wallace, B. A. *J. Membr. Biol.* **1992**, *129*, 109.
(23) Hladky, S. B.; Haydon, D. A. *Curr. Top. Membr. Transport* **1984**, *21*, 327.
(24) Rueda, M.; Navarro, I.; Prado, C.; Silva, C. *J. Echem. Soc.* **2001**, *4*, E139.
(25) Mauzeroll, J.; Bard, A. J. Manuscript in preparation.

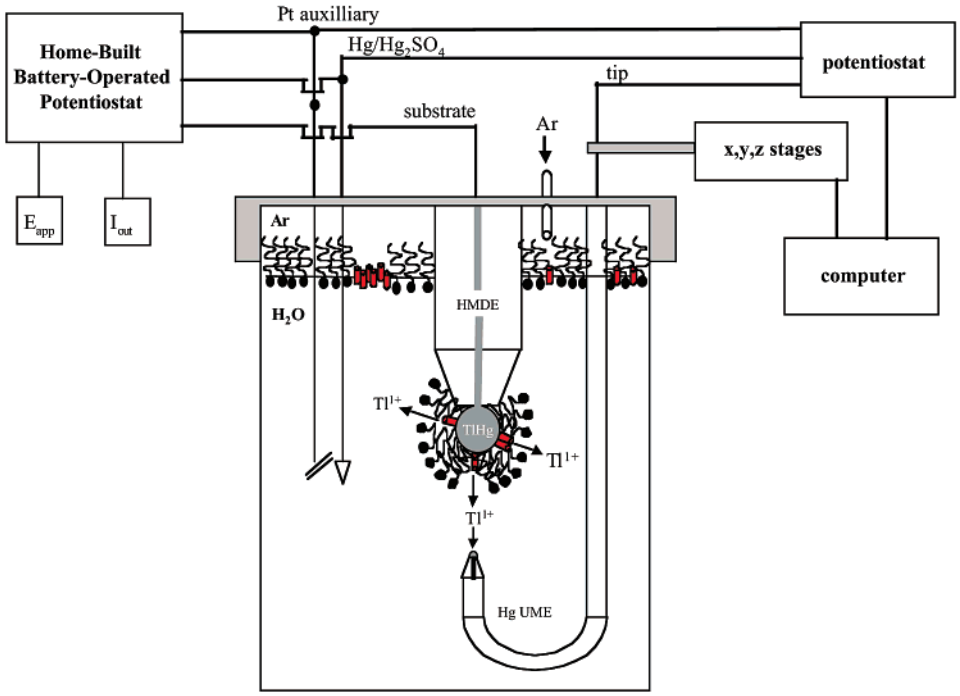

Figure 2. Experimental setup for the SG−TC experiments. A 750 mL cut beaker contains 250 mL of phosphate buffer and 250 μL of $TlNO_3$ stock solution, sealed with a Teflon cap that accommodates the HMDE, Hg/Pt submarine UME, Hg/Hg_2SO_4 reference, Pt auxiliary electrode, and gas inlet for Ar. The DOPC stock solution (35 μL) was added dropwise to form the monolayer at the Ar/solution interface. Gramicidin stock solution (15 μL) was added and stirred. Each new mercury drop had an area $A = 0.0139 \pm 0.0003$ cm^2. A battery-operated potentiostat and SECM setup were used to control the substrate and tip potential, respectively.

known distance. The reaction vessel was deaerated for 30 min, after which 250 μL of $TlNO_3$ stock solution was added. The voltammetric response of Tl(I) was then recorded at both tip and substrate.

The distance dependence of the tip transient response was evaluated by holding the substrate and tip at −1.1 V for 30 s, to form the substrate amalgam and to stabilize the tip current. The substrate potential was then switched to −0.75 V to oxidize the Tl amalgam. The tip, at −1.1 V, collected the released Tl(I) from the substrate for 100 s. The tip was then moved 25 μm further away from the substrate, and the experiment was repeated. This was carried out for several tip to substrate distances. A new amalgam HMDE was used for each distance, but the same Hg/Pt tip was used for the entire experiment. This implies that the drop on the tip was incorporating thallium, but saturation of the drop was not observed. Upon completion, an approach curve was recorded to assess the true tip to substrate distance. The solution was then purged with argon for 45 min.

The tip transient response was recorded for several tip to substrate distances with the amalgamated HMDE and the gramicidin−DOPC- and DOPC-modified amalgamated HMDE. To form the DOPC monolayer at the air/solution interface, 35 μL of the DOPC stock solution was added dropwise with a microsyringe. Upon contact, the drops spread at the interface and solvent evaporation was noticeable at the walls of the reaction vessel. The layer was left to organize on the solution surface for 30 min under an argon blanket.

The HMDE was used as the support for the DOPC and gramicidin−DOPC adsorbed monolayers. The adsorbed monolayers were prepared as previously reported.[19,26] The film spread at the air/solution interface was transferred to the bare and Tl amalgam HMDE by slowly passing it through the film. The quality of the film was then examined by looking at the decreased Tl(I) electrochemical response for a potential range that did not reach the first phase transition peak of the lipid layer (−1.3 V). Within −0.6 to −1.1 V, the monolayer is ion impermeable and the Tl(I) reduction at the HMDE should be significantly decreased by the presence of the DOPC layer as a result of blocking. At potentials more negative than −1.3 V, characteristic phase transition peaks appear and their voltammetric behavior has been studied.

The gramicidin half-channels were inserted into the DOPC air/solution interface by adding 15 μL of a 2.2 mM gramicidin stock solution to the solution in the cell. The solution and interface were then gently stirred for 5 min to allow uniform distribution of the gramicidin within the DOPC layer. The gramicidin−DOPC modified film was transferred to the HMDE in a similar fashion as described above. The voltammetric behavior of the gramicidin−DOPC film was also recorded prior to the SG−TC experiments; these are presented in the results section.

In the SG−TC experiments using the DOPC- and gramicidin−DOPC-modified substrates, the Tl/Hg amalgam was first formed for 30 s at the substrate. The films were then transferred to the amalgamated drop, and the drop was repositioned exactly at the same distance from the tip using a micromanipulator. A 30 s quiet time was applied to the tip prior to the oxidation of the amalgam. The substrate was then oxidized, and the tip transient response was measured. At the end of each experiment, an approach curve was recorded to ensure that the tip to substrate distance was conserved during the experiment. Each experiment used a new mercury drop (area $A = 0.0139 \pm 0.0003$ cm^2).

3. Results and Discussion

3.1. Substrate Generation−Tip Collection Experiments. 3.1.1. Formation of Hg/Pt Submarine Electrodes. A 25 μm Hg/Pt UME formed upon touching a Pt UME to Hg (Figure 3a). The 25 μm Pt "submarine" electrode was poised at −1.1 V and approached the HMDE in a deaerated phosphate buffer (pH = 7) at 1 μm/s. This Hg/Pt UME was characterized by cyclic voltammetry and SECM feedback experiments. As shown in Figure 3b, a 0.5 V overpotential for hydrogen evolution was observed in deaerated phosphate buffer (pH = 7) following the Hg deposition onto Pt. The response presented in Figure 3b suggests full coverage of the Pt by the Hg. The presence of uncovered Pt regions would have resulted in a microarray voltammetric response for hydrogen evolution

(26) Nelson, A.; Benton, A. *J. Electroanal. Chem.* **1986**, *202*, 253.

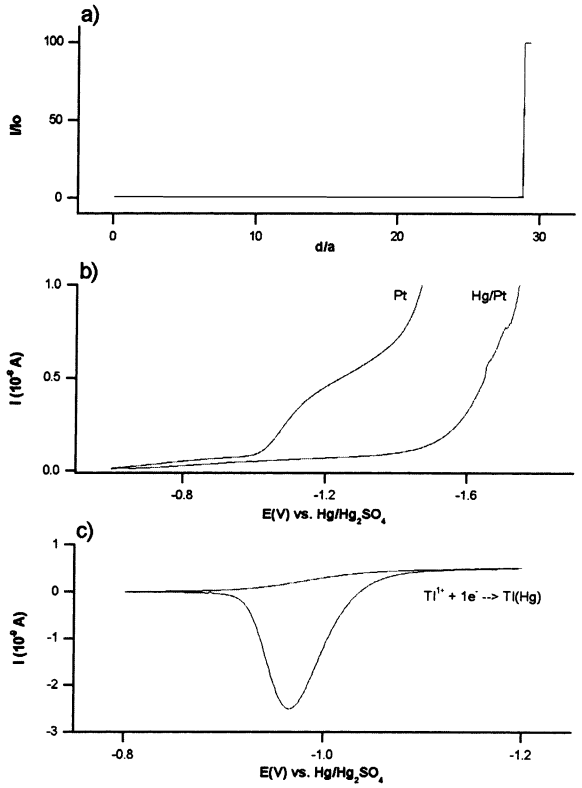

Figure 3. Formation and characterization of the Hg/Pt submarine electrode. (a) The Pt submarine electrode in phosphate buffer (pH = 7) as it approached the HMDE while poised at −1.1 V vs Hg/Hg_2SO_4. Upon contact with the HMDE, a hemispherical mercury layer is deposited onto the Pt UME. (b) Hydrogen evolution at the Pt and Hg/Pt submarine UME in phosphate buffer. (c) Voltammogram of the 10^{-4} M Tl(I) at the Hg/Pt submarine electrode in phosphate buffer.

on Pt. The extension of the potential window allowed the detection of Tl(I) electrochemistry at the SECM tip (Hg/Pt UME) (Figure 3c). The voltammogram presents a stable steady-state current for the Tl(I) reduction and a characteristic stripping peak for the oxidation of the Tl amalgam.

The Hg/Pt submarine UME showed good positive feedback with $Ru(NH_3)_6^{2+}$ when it approached a HMDE (Figure 4). The experimental approach curve fit the theory developed by Mandler et al.[27] for a hemispherical UME. The analytical approximation for the positive feedback equation (±1%) (normalized current vs distance) of a hemispherical UME is:

$$i_t/i_{t,\infty} = 0.873 + \ln(1 + L^{-1}) - 0.20986 \exp[-(L - 0.1)/0.55032] \quad (1)$$

where i_t is the tip current, $i_{t,\infty}$ is the steady-state current when the tip is far from the substrate, and L is the ratio of the tip to substrate spacing and the active electrode radius (12.5 μm) (d/r_0).

The response is significantly different from that predicted for a disk:[28]

$$i_t/i_{t,\infty} = 0.68 + 0.7838/L + 0.3315 \exp[-(1.0672/L)] \quad (2)$$

The tip shape affects the approach curves because of proportional differences in lateral and normal diffusion to the tip. The normalized current for a hemispherical tip is smaller than that of the disk electrode at short distances (Figure 4). This agrees with previously reported studies of gold spherical UMEs prepared by self-assembly of gold nanoparticles.[29] For a disk UME, the diffusion of the electroactive species normal to the tip outweighs the radial diffusion component as the tip approaches a conductive substrate. The hemispherical UME protrudes from the glass sheet and is more sensitive to lateral diffusion. As the tip approaches the conductive substrate, the current measured will systematically be smaller than that at the disk UME.

The deposited Hg hemisphere was stable and did not change surface area upon subsequent contact with the HMDE because of liquid trapping between the two mercury surfaces.[25] This repulsion between two mercury surfaces has previously been reported and is said to depend on the symmetry of the two mercury surfaces, the charge, and the presence of adsorption processes.[30] The presence of a trapped layer was observed as a change of slope in the approach curves at very short distances in the SECM positive feedback experiments. In fact, a 25 μm size UME approaching a Hg pool could trap and push into the pool a 0.56 μm thick water layer.[31] Also, voltammograms recorded following successive contacts of the UME with the HMDE presented no significant change in the steady-state current, showing no appreciable change in the UME electrode area.

3.1.2. Tip Transient Response in Collection Experiments. The tip transient response for the collection of the Tl(I) generated at a bare Tl(Hg) electrode is presented in Figure 5. The collection response depends on the Tl(I) concentration profile generated at the substrate. Since the substrate amalgam concentration, area, and applied potential for oxidation remain constant for all experiments, the generated concentration profile is entirely governed by the diffusion layer thickness. At short collection times, the tip current remains at baseline level until the generated Tl(I) has diffused from the substrate to the tip. For large tip to substrate separation, the diffusion time is long and the collection of Tl occurs later than for small separations. As discussed below, the tip collection current follows an error function complement relationship for the short time regime and reaches a maximum because of depletion of Tl from the source amalgam. At small separations, the concentration profile is compact and the slope of the collection response is steeper than for larger separations. The transient peak maximum is smaller and generally tends to shift to longer times at larger tip to substrate distances.

The amalgam formation was limited to 30 s so that the surface properties of the Hg drop would not be altered significantly. The source amalgam is therefore exhausted rapidly during the transient collection at the tip. This leads to the formation of the peak maximum and the return of the tip current to the baseline value. The baseline current for the reduction of Tl(I) at the UME is nonzero due to the presence of some dissolved Tl(I) in the buffer solution. Because of the restrictions imposed by the gramicidin DOPC monolayer, it was impossible to conduct this experiment in the absence of background Tl(I).

3.1.3. Tip to Substrate Distance Evaluation. The tip to substrate distance dependence of SG−TC experi-

(27) Selzer, Y.; Mandler, D. *Anal. Chem.* **2000**, *72*, 2383.
(28) Arca, M.; Bard, A. J.; Horrocks B. R.; Richards, T. C.; Treichel, D. A. *Analyst* **1994**, *119*, 719.
(29) Demaille, C.; Brust, M.; Tsionsky, M.; Bard, A. J. *Anal. Chem.* **1997**, 69, 2323.
(30) Usui, S.; Yamasaki, T.; Simoiizaka, J. *J. Phys. Chem.* **1967**, *71* (10), 3195.
(31) Mirkin, M. V.; Bard, A. J. *J. Electrochem. Soc.* **1992**, *139*, 3535.

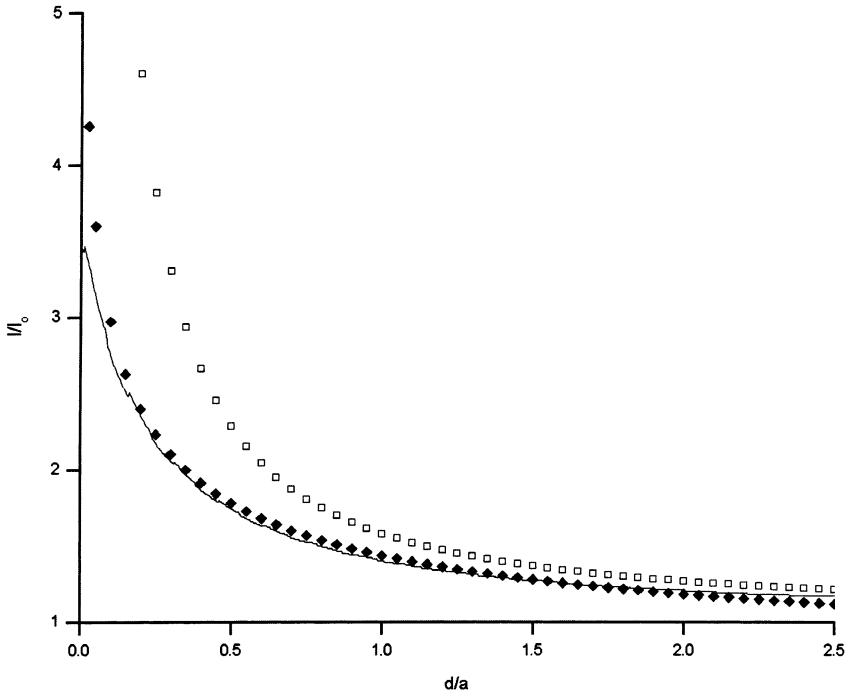

Figure 4. Positive feedback SECM curve fitting of (line) the Hg/Pt submarine electrode approach curve to (♦) hemispherical SECM theory and (□) disk SECM theory for a 2 mM hexamineruthenium chloride solution in phosphate buffer (pH = 7). The Hg/Pt UME approached the HMDE.

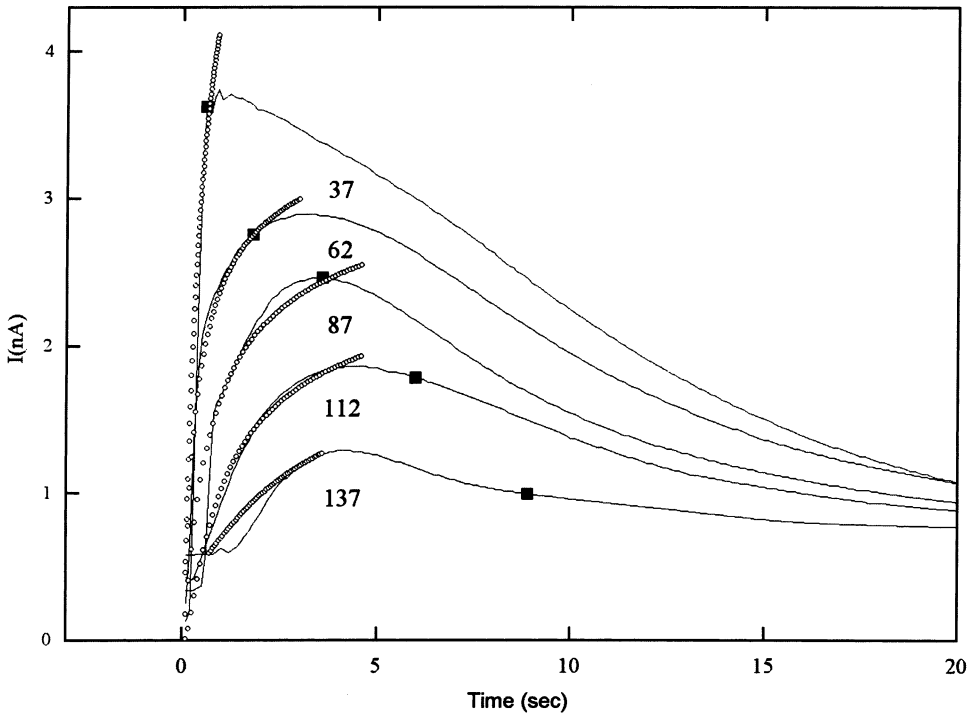

Figure 5. (line) Tip transient response for the collection of generated Tl(I) for different tip to substrate separations. The distances were evaluated by curve fitting the final approach curve in 10^{-4} M $TlNO_3$ to the negative feedback hemispherical SECM theory. The ○ symbols represent the error function complement fits performed from a nonlinear least-squares fitting based on the LV algorithm. The ■ symbols represent the time extracted from the diffusion layer thickness equation: $\Delta = \sqrt{(2Dt)}$.

ments for Tl(I) collection at the Tl/Hg HMDE is reported in Figure 5. A calibration curve for the distances reported in the figure was obtained from an SECM negative feedback approach curve. To obtain this curve, the tip was poised at the potential for Tl(I) reduction in the electrolyte as it approached the HMDE (that was disconnected and so at open circuit). The SECM approach curve was fit to the negative feedback approximation equation for a hemispherical electrode:[27]

$$i_t/i_{t,\infty} = 0.39603 + 0.42412L + 0.09406L^2 \quad (3)$$

The tip to substrate distance was evaluated from the fit. In the present case, the adjustment for zero distance is minimal because of the known position of initial contact of the tip to the HMDE during Hg/Pt UME formation.

Table 1. Tip to Substrate Distance Evaluation Using an Error Function Complement Approximation[a]

erfc argument	$\Delta_{erfc(x)}$ (μm)	Δ_{SECM} (μm)
0.431	27	37
1.103	70	62
1.384	88	87
1.765	112	112
2.282	144	137

[a] The rising part of the transient response for Tl(I) collection at the tip was fitted to an error function complement. The tip to substrate separation (Δ) was extracted from the error function complement argument. This distance was compared to the one obtained from the SECM calibration.

There is however some uncertainty in the determination of the contact distance and in the thickness of the Hg film that can account for some error in distance.

The tip to substrate distances extracted from SECM fits are presented in Table 1. These distances represent the thickness of the solution layer that the Tl(I) generated at the HMDE must cross to reach the UME. The diffusion layer thickness, Δ, is usually given by an approximation such as $\Delta = (2Dt)^{1/2}$, where D is the diffusion coefficient (cm^2/s) and t is the time (s). In the present collection experiments, this approximation is not a good representation of the actual distance. The diffusion times calculated from the diffusion layer thickness equation at the tip to substrate distances reported in Figure 5 are represented by the squares in this figure. Experimentally, the initial collection of Tl(I) occurs much sooner than that predicted by the diffusion layer approximation.

The concentration profile, $C_0(x,t)$, of Tl(I) generated at the HMDE is governed by spherical diffusion. However, the close spacing of the tip to the much larger HMDE allows us to approximate the diffusion of the generated Tl(I) as linear. For the unmodified amalgam HMDE system, the generated concentration profile of Tl(I) from a pre-existing Tl(Hg) amalgam is treated as a double potential step chronoamperometric problem (see the Appendix). The concentration profile generated at the HMDE and detected by the tip is given by:[32]

$$C_0(x,t) = C_0^* \operatorname{erfc}\left[\frac{x}{2(D_0 t)^{1/2}}\right] \quad (4)$$

where C_0^* is the bulk concentration of Tl(I) in solution before the amalgam formation, x is the tip to substrate distance, and t is a time variable that considers the reversal time as the zero time. This approximation was also used by Engstrom et al. in earlier work.[7] They showed that the general shape, amplitude, and time delay of this equation predicted their experimental results for tip to substrate spacings greater than 10 μm. Here the tip current is given by the usual UME equation, with the concentration obtained from eq 4, that is:

$$i_t = 4nFD_0C_0(x,t)r_0 \quad (5)$$

The tip to substrate distance was evaluated by fitting the rising portion of the curves in Figure 5; these are reported in Table 1 where they are compared to the distances evaluated from the SECM approach curves. The values obtained by this approximation are better than those derived from a simple diffusion layer approximation. At shorter distances, the approximation in eq 4 does not hold as well because of feedback effects.

(32) Bard, A. J.; Faulkner, L. R. *Electrochemical Methods*, 1st ed.; John Wiley & Sons: New York, 1980; p 180.

3.2. Monolayer Formation and Characterization. Figure 6 presents the characterization of the DOPC films by voltammetry. Within the range of −0.6 and −1.1 V, the DOPC monolayers adsorbed on mercury are generally ion impermeable. The Tl(I) voltammetric response for a DOPC-modified HMDE is therefore significantly smaller compared to the bare HMDE signal (curves b and a, respectively). DOPC monolayers adsorbed on mercury show a small density of defects that account for the residual Tl(I) signal observed in Figure 6b.[33] Beyond −1.1 V and up to the onset of the first phase transition peak (Figure 6d), the DOPC layer becomes more permeable to metal ions with applied potential. Beyond this first phase transition peak, the density of defects increases with potential. Molecularly, the lipid monolayer reverts to a two-phase system of a thick and a thin monolayer.[34] The second phase transition peak represents the growth and coalescence of defects formed in the first phase.[20] If the potential window is expanded further to more negative potentials, a third peak indicating the DOPC layer being displaced from the mercury surface appears. In this paper, the experiments were restricted to the potential window where the DOPC adsorbed layer was impermeable to metal ions.

The insertion of gramicidin in the DOPC monolayer increases the permeability of Tl(I) ions, and this led to an increase in the voltammetric response (Figure 6c). The response resembles that of a process determined by a kinetically driven process. The orientation of the gramicidin−DOPC modified monolayer is governed by the hydrophobicity of the mercury.[34] The carbon tails of the DOPC face the metal surface while the headgroup is in solution. This orientation is supported by experimental results comparing the potential of zero charge of the DOPC layer on mercury to the surface potential of condensed phosphatidylcholine (PC) monolayers at the air−water interface.[33] Theoretical calculations also predict that within the potential range −0.6 to −1.1 V phospholipid molecules in a monolayer should have their tails facing the mercury and the headgroups facing the electrolyte.[34] This arrangement prevents multilayer formation from repeated touches of the monolayer on the HMDE with the film at the air/water interface.

The particular orientation of the DOPC layers influences the organization of the $\beta^{6.3}$ gramicidin helix in the layer. At the end of each gramicidin A, there are four tryptophan residues as shown in Figure 1. These residues are polarizable and capable of hydrogen bonding to the polar headgroup of the lipid and with the water in solution.[35−38] The gramicidin half-channels are therefore probably closer to the electrolyte solution than the mercury. A similar arrangement is observed for gramicidin B and C that have one fewer tryptophan residue.

3.3. SG−TC of Thallium(I) in Gramicidin Channels. Collection experiments of Tl(I) at the Hg/Pt UME with generation at a Tl amalgam/HMDE for bare, DOPC-modified, and gramicidin−DOPC-modified Tl/HMDE are reported in Figure 7. As mentioned earlier, the Tl amalgam is first formed on the HMDE prior to the adsorption of the DOPC and gramicidin−DOPC layers onto the substrate. Upon application of the potential capable of oxidizing Tl at the substrate, a switching transient is observed for a

(33) Bizzotto, D.; Nelson, A. *Langmuir* **1998**, *14*, 6269.
(34) Rueda, M.; Navarro, I.; Ramirez, G.; Prieto, F.; Prado, C.; Nelson, A. *Langmuir* **1999**, *15*, 3672.
(35) Wallace, B. A. *Annu. Rev. Biophys. Chem.* **1990**, *19*, 127.
(36) Killian, J. A. *Biochim. Biophys. Acta* **1992**, *1113*, 391.
(37) Hu, W.; Lee, K. C.; Cross, T. A. *Biochemistry* **1993**, *27*, 7035.
(38) Wallace, B. A. *Adv. Exp. Med. Biol.* **1996**, *398*, 607.

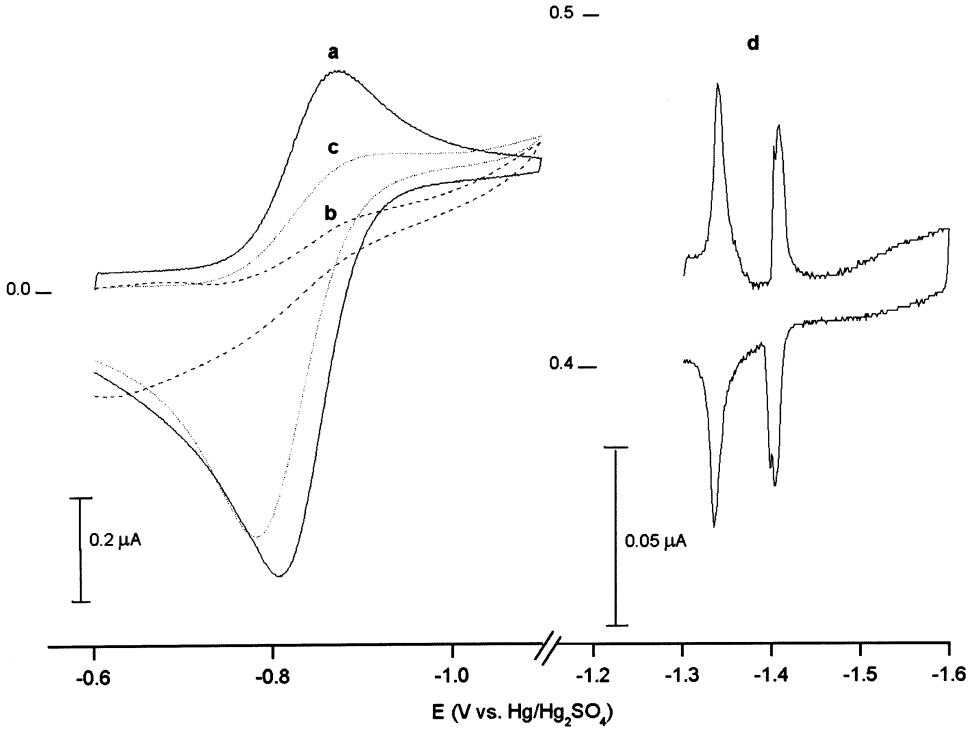

Figure 6. The voltammetric response of (a) bare HMDE, (b) DOPC-modified HMDE, and (c) gramicidin−DOPC-modified HMDE in 10^{-4} M $TlNO_3$ in phosphate buffer for a 50 mV/s scan rate. (d) The voltammetric response of the DOPC-modified HMDE system outlining the reversible first and second monolayer transitions in 10^{-4} M $TlNO_3$ in phosphate buffer for a 50 mV/s scan rate.

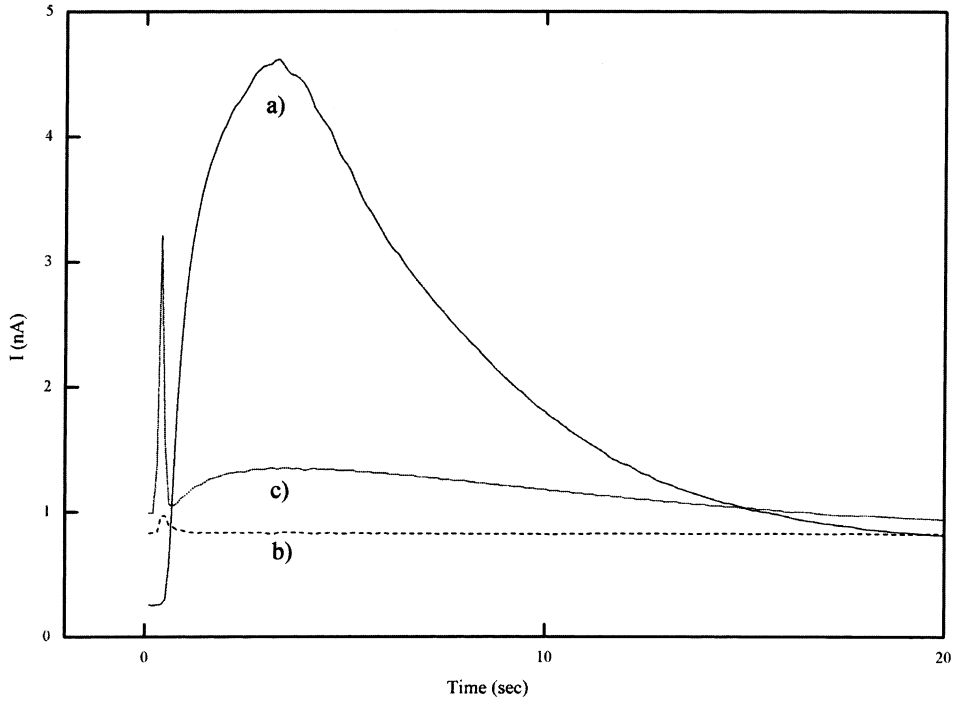

Figure 7. SG−TC tip transient response for the (a) bare Tl/HMDE, (b) DOPC-modified Tl/HMDE, and (c) gramicidin−DOPC-modified Tl/HMDE with a tip to substrate distance of 87 μm. The Tl/Hg amalgam was formed for 30 s, and the measurements were performed in 10^{-4} M $TlNO_3$ in phosphate buffer. These results were obtained with a different Hg/Pt UME than the results presented in Figure 5.

few hundred milliseconds. The collection response was then recorded at a tip positioned 87 μm away from the substrate. All transient responses presented in Figure 7 were recorded with the same tip (a different one than that used to collect the distance transients in Figure 5).

The trend recorded for the tip transient response for the bare, DOPC-modified, and gramicidin−DOPC-modified systems (Figure 7a−c, respectively) is similar to that observed in the voltammetry experiments (Figure 6a−c). The bare electrode has the steeper slope and the highest maximum. The background current for the bare electrode is lower because this run was made just after degassing. The results for DOPC-modified and gramicidin−DOPC-modified systems were recorded following monolayer formation and insertion of gramicidin into the layer. Although an Ar blanket was maintained for the entire

experiment, some limited oxygen contamination could explain the small increase in background current for these systems.

The DOPC-modified system was totally blocking. This indicates that the defects observed in Figure 6b do not affect the response significantly and present a sensitivity limitation of the technique. The defects in Figure 6b were still present, but the Tl(I) transport through them was undetectable by the Hg/Pt tip because it addressed only a small portion of the substrate and there was a background current of Tl(I) in the solution. The introduction of gramicidin increased the passage of Tl(I) through the monolayer, and this was detected. The Tl(I) released through the gramicidin channels (Figure 7c) showed a smaller slope and lower maximum. The response is broader and peaks at nearly the same time as compared to that of the bare Hg. The decay slope is also not as steep, consistent with a slower release of the Tl into solution. These results were reproduced in two additional experiments at similar tip to substrate distances and showed good agreement with the results presented.

The generation of Tl(I), transport across gramicidin, and subsequent collection at the tip from the solution can be viewed as a rate controlled by diffusion. The concentration profile is governed by mass transfer through the solution and the rate at which the generated Tl(I) is transported across the gramicidin channels (which we treat below as a heterogeneous kinetic process). We assume semi-infinite linear diffusion to calculate the concentration profile of the generated Tl(I). Linear diffusion is a reasonable model for this experiment because the tip to substrate distance is much larger than the spacing between two channels but small with respect to the HMDE radius. To obtain the concentration profile[31] of the generated Tl(I), we use the diffusion equation and the initial, semi-infinite, and flux balance conditions along with the heterogeneous rate constant as used in the irreversible potential step problem[39] to yield the following Laplace transformation:

$$\bar{C}_0(x,s) = \frac{k_{het} C_{Tl(I)}^*}{\sqrt{D}} \left\{ \frac{e^{-x\sqrt{(s/D)}}}{s[(k_{het}/\sqrt{D}) + \sqrt{s}]} \right\} \quad (6)$$

With simple variable substitution and the inverse transformation of eq 6,[40] we obtain:

$$C_0(b,t) = C_{Tl(I)}^* \left\{ \mathrm{erfc}\left(\frac{b}{2\sqrt{t}}\right) - e^{ab}\, e^{a^2 t}\, \mathrm{erfc}\left(a\sqrt{t} + \frac{b}{2\sqrt{t}}\right) \right\} \quad (7)$$

where $a = k_{het}/D^{1/2}$, $b = x/D^{1/2}$, k_{het} is the apparent heterogeneous rate constant (cm/s) for the transport of Tl(I) through the channels, D is the diffusion coefficient of the generated species (cm^2/s) in solution, x is the tip to substrate separation (cm), and t is the diffusion time (s). $C_{Tl(I)}^*$ is the concentration of Tl(I) in the drop following the film formation. This concentration is assumed constant and is related to the amalgam formation time. From eqs 5 and 7, the UME collection tip current for the Tl(I) generated at the HMDE that moves through the gramicidin channels and diffuses across the solution gap is:

$$i_t = 4nFr_0 D C_{Tl(I)}^* \left\{ \mathrm{erfc}\left(\frac{b}{2\sqrt{t}}\right) - e^{ab}\, e^{a^2 t}\, \mathrm{erfc}\left(a\sqrt{t} + \frac{b}{2\sqrt{t}}\right) \right\} \quad (8)$$

Equation 8 has two unknowns, the concentration of Tl(I) on the drop following film formation and the heterogeneous rate constant. The k_{het} was extracted based on a two-parameter fit from the rising part of the SG−TC response of the gramicidin−DOPC-modified system using a nonlinear least-squares fitting based on the Levenberg−Marquardt (LM) algorithm. The background Tl(I) current was subtracted from the collection response; the switching transient and depletion region of the substrate were omitted from the fit. From the fitting results in Figure 8, $k_{het} = 2.8\ (\pm 0.1) \times 10^{-4}$ cm/s for $x = 87\ \mu$m, and $D = 2 \times 10^{-5}$ cm^2/s. The error function complement argument is very small in this fitting, and so the expression is linear in this domain.

Significant work and models have been put forth to elucidate the transport mechanism of monovalent cations from the bulk solution through gramicidin.[21,22,41] These are based on a porous layer model where the charge transfer takes place at microscopic inhomogeneities while the rest of the electrode surface is covered by a blocking film.[42] Molecularly, monovalent cations are partially dehydrated upon coordination with the carbonyls of the tryptophan residues at the mouth of the channel. They are then transported through the channel along with water molecules. The nature of our experiments does not allow us to discuss the validity of these models. Our results do enable us to compare the heterogeneous rate constants extracted from our work with reported ones.

Most of the electrochemical methods used to study the transport process[17,21,36] looked at the reduction of Tl(I) for the transport of an ion from the bulk solution to the HMDE. The heterogeneous rate constant ($k_{het} = 8 \times 10^{-3}$cm/s) derived from quasi-steady-state chronoamperometric measurements is larger than the one reported here.[17] The transport process for the stripping experiment from Hg may well be different from that when the ion is transported from the bulk aqueous solution. Once oxidized from the substrate, the Tl(I) must be aquated and transported through the gramicidin. Once at the half-channel, the ion does not benefit from the carbonyl interactions at the mouth of the channel. The transport of Tl(I) from the HMDE to the bulk solution might therefore be more energetically costly and thus result in a smaller apparent heterogeneous rate constant. If there is asymmetry in the activation barrier of the half-channels, it would be interesting to compare the rates obtained for a similar system with a full channel (Figure 1) where the activation barrier should be more symmetric. Differences in rates in such experiments might then reveal some potential dependence of the rate constant for the Tl oxidation. A recent report by Guidelli,[41] however, suggests that the flux of Tl(I) from the gramicidin−DOPC-modified Tl/HMDE to the solution is potential independent and mainly controlled by diffusion, based on linear scan voltammetry performed on a system similar to that used in the present work.

(39) Bard, A. J.; Faulkner, L. R. *Electrochemical Methods*, 2nd ed.; John Wiley & Sons: New York, 2001; p 192.
(40) Carslaw, H. S.; Jaeger, J. C. *Conduction of Heat in Solids*, 2nd ed.; Clarendon Press: Oxford, 1959.
(41) Becucci, L.; Moncelli, M. R.; Guidelli, R. *Biophys. J.* **2002**, *82*, 852.
(42) Amatore, C.; Savéant, J. M.; Tessier, D. *J. Elec. Anal.* **1983**, *147*, 39.
(43) Ketchem, R. R.; Hu, W.; Cross, T. A. *Science* **1993**, *261*, 1457.
(44) Ketchem, R. R.; Lee, K. C.; Huo, S.; Cross, T. A. *J. Biomol. NMR* **1996**, *8*, 1.

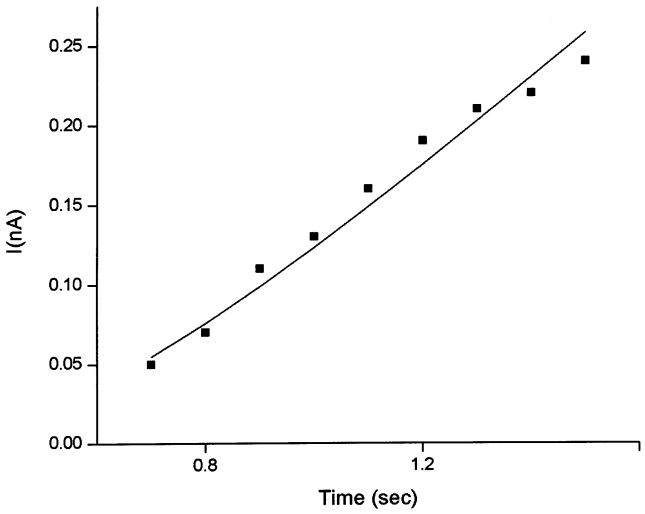

Figure 8. Fitting of the rising part of the gramicidin−DOPC-modified transient response to eq 8. The nonlinear fitting used the LM algorithm to extract $P1 = k_{het}/\sqrt{D} = 0.06347 \pm 0.00153$. The reduced Chi square (1.3268E−22) was minimized. The fit yielded $k_{het} = 2.8\ (\pm 0.1) \times 10^{-4}$ cm/s for $x = 87\ \mu$m, and $D = 2 \times 10^{-5}$ cm^2/s.

4. Conclusions

A Hg/Pt submarine UME tip was formed through simple contact of a Pt UME with a HMDE and used as a detector for Tl(I) (which serves as a surrogate for K^+) in SECM. The tip transient collection response for different tip to substrate distances was evaluated using Tl(I) generated at an amalgamated HMDE. Transfer of DOPC and gramicidin−DOPC monolayers onto the amalgamated HMDE from the air/solution interface was carried out, and the collection of released Tl(I) across gramicidin at the Hg/Pt submarine electrode was achieved. Comparison of substrate (HMDE) generation−tip collection behavior of the bare amalgamated, DOPC-modified, and gramicidin−DOPC-modified HMDE confirmed the selective transport of Tl(I) across gramicidin. Finally, an apparent heterogeneous rate constant for the transport of Tl(I) from the HMDE into the bulk was obtained.

To our knowledge, this is the first time that SECM has been used in an amperometric mode to control and monitor ion transport across ion channels. We plan to perform similar studies on living systems having complete phospholipid bilayers and biologically functional channels.

Acknowledgment. This work was funded by the National Science Foundation (NSF) Grant Number CHE0109587 (UT), the Ministry of Science and Technology (Madrid) for Project BQU2001-3197, and a grant from the Andalusian Research Plan (Seville). We appreciate the help and advice of Dr. Z. Ding and Dr. F. F-R. Fan.

Supporting Information Available: A graph showing the magnitude of the erf response in comparison to that of erfc. This material is available free of charge via the Internet at http://pubs.acs.org.

Appendix

The generation of Tl from a nonmodified amalgam HMDE and collection experiments presented in Figure 5 are treated as a double potential step chronoamperometric problem. During the first potential step, a Hg−Tl amalgam is formed by bulk electrolysis of a Tl(I) solution until the reversal time, τ, when the potential is stepped to oxidize the amalgam back to Tl(I). The generated Tl(I) is then collected at the nearby UME.

The diffusion of Tl(0) in the mercury is identical to solution diffusion since the diffusion coefficients of both Tl(0) and Tl(I) are of the same order of magnitude. The concentration profile, $C_0(x,t)$, of Tl(I) generated at the HMDE is governed by spherical diffusion. However, the close spacing of the tip to the much larger HMDE and the time scale of the experiment allow an approximation of the diffusion of the generated Tl(I) as linear. From the theoretical treatment of the double potential step chronoamperometry problem, the concentration profile of the Tl(I) generated at the HMDE and subsequently collected at the UME is given by:[32]

$$\frac{C_0(x,t)}{C_0^*} = 1 - \left(\frac{1}{1+\xi\theta'}\right)\mathrm{erfc}\left(\frac{x}{2[D_0 t]^{1/2}}\right) + S_\tau(t)\left(\frac{\xi\theta''}{1+\xi\theta''} + \frac{\xi\theta'}{1+\xi\theta'}\right)\mathrm{erfc}\left(\frac{x}{2[D_0(t-\tau)]^{1/2}}\right) \quad \text{(A1)}$$

where D_0 is the diffusion coefficient of Tl(I) in solution; x is the tip to substrate distance; t is the time at the start of the electrolysis step; $S_\tau(t)$ is a step function that is unity after reversal and zero before the reversal time; τ is the reversal time; $C_0^* = C_{Tl}(x,0)$, the bulk concentration of Tl(I) in solution before electrolysis; and $\xi = \sqrt{(D_0/D_r)} \approx 1$.

Since both diffusion coefficients are on the same order of magnitude, for $t < \tau$

$$\theta' = C_{Tl}'(0,t)/C_{Tl,Hg}'(0,t) \quad \text{this ratio is very small}$$

and for $t > \tau$

$$\theta'' = C_{Tl}''(0,t)/C_{Tl,Hg}''(0,t) \quad \text{this ratio is very large}$$

Based on the assumptions stated above, eq A1 can then be reduced to:

$$\frac{C_0(x,t)}{C_0^*} = \mathrm{erf}\left(\frac{x}{2[D_0 t]^{1/2}}\right) + \mathrm{erfc}\left(\frac{x}{2[D_0(t-\tau)]^{1/2}}\right) \quad \text{(A2)}$$

For the experimental times and distances studied in the generation−collection experiments, the error function argument in eq A2 is very small. The erf response represents only 5% of that of erfc and can be neglected. A graph of this is available in the Supporting Information. The error function term is therefore neglected so that:

$$\frac{C_0(x,t)}{C_0^*} = \mathrm{erfc}\left(\frac{x}{2[D_0(t-\tau)]^{1/2}}\right) \quad \text{(A3)}$$

This yields eq 4 in the text. The assumptions made do not hold strictly. At longer distances, as seen in Figure 5, the theoretical curve does not fit the experimental response well, although it does allow an adequate estimation of the tip to substrate distances in our experiments (Table 1). For experiments where the distances are larger, the erf term should be included.

LA0262710